How Reliable Are Computer Simulations for RF Power Deposition? An Experimental Verification of Numerical Simulations

S. Li[1], S. Wang[1], and J. Shen[1]

[1]National Institutes of Health, Bethesda, Maryland, United States

INTRODUCTION

Numerical simulation methods, mainly Time-Domain Finite-Difference (FDTD) and Finite Element Method (FEM), have been extensively used in the past decade to study B_1 field distribution and RF safety, particularly for high field applications. The simulated B_1 field and imaging characteristics are in good agreement with experimental measurements [1-4]. Although many simulations have calculated the RF power deposition inside 3-D human head models [5-8], to the best of our knowledge, the calculated data have not been experimentally verified. In this study, we performed numerical simulations and experimental measurements at 4.7 Tesla of the RF power deposition inside several different phantoms using the same coil/phantom setup. Results of this comparison between the simulated and experimental data may make researchers more confident in their ability to use numerical simulation for RF safety evaluations.

METHODS

Coil and phantoms: A shielded, 12-rung one-port linear high-pass birdcage coil was built with coil dia. = 4.0 cm and shield dia. = 17.8 cm. Copper tape was used to make rungs (2.54-cm wide) and end-rings (1.90-cm wide). The overall height of the coil was 16.5 cm. Three chip capacitors were placed in parallel at each open slot of the end-rings, and the coil was tuned to 200.6 MHz. The 1st phantom was a sphere (dia. = 3.5 cm) filled with distilled water only (no loading effect). The 2nd, 3rd, and 4th phantoms were spheres (dia. = 10.1cm) filled with 25, 50, and 75 mM NaCl solution, respectively (see Table).

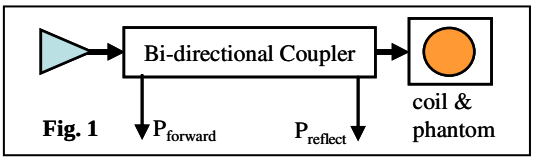

Fig. 1

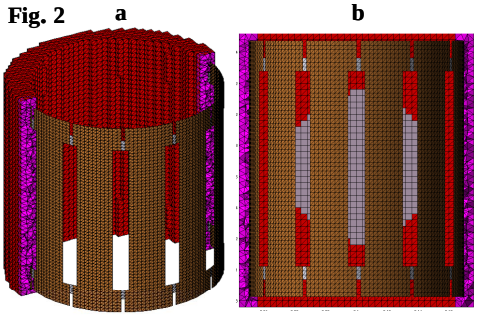

Fig. 2

Experimental measurement: The RF power deposition inside each phantom was measured using the method defined by the National Electrical Manufacturers Association (document MS8) and the International Electrotechnical Commission (IEC 60601-2-33). The method is illustrated in Fig. 1 and summarized by the formulas:

$$P_{coil} = P_{forward\ 1} - P_{reflect\ 1} \text{ (using unloaded phantom 1)}$$

$$P_n = P_{forward\ n} - P_{reflect\ n} - P_{coil} \text{ (using phantom n, n = 2, 3, and 4)}$$

where P_{coil} is the power dissipated by the coil itself—including coil resistive loss and radiation loss—and P_n is the power absorbed inside the n-th phantom. All power levels were measured at a condition of 180° flip angle with a 2-ms rectangular pulse at the coil center. The B_1^+ field map was also experimentally mapped using a spin-echo based imaging method by acquiring two images at different excitation flip angles [9].

Numerical simulation: A FDTD/FEM hybrid method [10] was applied: the birdcage coil was modeled with unstructured tetrahedral meshes and the FEM method (Fig. 2a), and the rest of the space and the phantoms were modeled with 3-mm cubical Yee cells and the FDTD method. The region colored pink denotes the cross-sectional view of the tetrahedral mesh near the coil conductors (brown). Spherical phantoms were modeled with 3-mm cubical Yee cells (in gray, Fig. 2b). The coil was tuned to 200.6 MHz by adjusting 72 capacitances with phantoms. Although the phantoms can also be modeled with unstructured tetrahedral mesh, most human models are voxel-based and Yee cells are more common in practical phantom modeling. According to the concentration of the NaCl solution, the conductivities of the numerical phantoms were 0.22 S/m, 0.44 S/m, and 0.66 S/m at 200 MHz respectively. The calculated B_1^+ intensity at the center of the phantoms was normalized to 5.87 μT (180° flip angle with a 2-ms rectangular pulse). The corresponding power deposition was obtained by integrating the electrical power from all Yee cells inside the phantom region at the normalized condition.

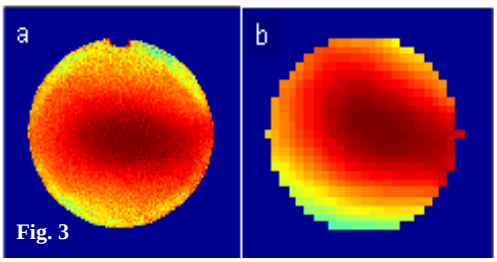

Fig. 3

Phantom number	2	3	4
NaCl concentration (mM)	25	50	75
Conductivity (S/m)	0.22	0.44	0.66
Measured power (Watt)	2.3	4.5	6.6
Simulated power (Watt)	1.7	3.5	5.6

RESULTS AND DISCUSSION

Fig. 3 shows the experimentally measured B_1^+ field map (a) and the simulated B_1^+ field map (b) inside the phantom with 75 mM NaCl. The field patterns are in good agreement. Results from experimentally measured and simulated RF power depositions inside the three different phantoms are shown in the Table. The results show that the simulated values are reasonably close to the experimentally measured results, especially for the phantoms with higher NaCl concentrations. The measured power absorption under experimental conditions was 35%, 28%, and 18% higher than the simulated data for phantoms 2, 3, and 4, respectively. These differences may be due to several factors. For example, accumulated errors in the measurement of peak-to-peak voltage and power attenuation of cables and the bi-directional coupler are inevitable. Also, conductivity in the real phantom and in the computer phantom models might not be identical. As shown in the Table, the relative power increases using the two methods are much closer to each other. Since the range of conductivities of the phantoms includes those of most human tissues at the same RF frequency, these preliminary results demonstrate that the RF power deposition calculated using numerical simulations is reasonably close to the measured power level, and thus provides additional evidence that this method can be used as a reliable reference for RF safety evaluations.

REFERENCES

1. CM Collins et al. Magn Reson Med 2002;47:1026; **2.** J Wang et al. Magn Reson Med 2002;48:362; **3.** TS Ibrahim et al. Magn Reson Med 2005;54:683; **4.** TS Ibrahim et al. NMR in Biomed 2007;20:58; **5.** CM Collins et al. Magn Reson Med 1998;40:847; **6.** Z Wang et al. J Magn Reson Imag 2007;26:437; **7.** UD Nguyen et al. IEEE Tans Biomed Eng 2004;51:1301; **8.** TS Ibrahim et al. J. Magn Reson Imag 2007;26:1362; **9.** R. Stollberger et al. Magn Reson Med 1996;35:246. **10.** S Wang et al. Phys. Med. Biol. 2008;53:2677.